Kovove Mater. *64* *2026* *85–93*
DOI: *10.31577/km.2026.2.85*

Investigation of the influence of temperature and notch bottom through experimental and numerical integration

Sihem Achouri[1]*, Mounira Bourebia[1], Soumaya Meddah[1]

[1] *Research Center in Industrial Technologies CRTI, P.O. Box 64, Cheraga 16014 Algiers, Algeria*

Received 4 February 2026, received in revised form 15 March 2026, accepted 15 May 2026

Abstract

This study investigates the combined effect of temperature and notch depth on the Charpy impact toughness of API 5L X70 pipeline steel using an experimental approach coupled with statistical modeling. A 2^2factorial design of experiments was implemented to evaluate the influence of two factors: temperature (T), coded as X_1, and notch depth (Nd), coded as X_2. Charpy V-notch impact tests were performed according to the experimental matrix defined by the design of experiments, and the absorbed fracture energy (U) was measured for each condition. The results indicate that the notch depth has a more significant influence on the absorbed energy than temperature within the studied range. Furthermore, the fracture energy increases within creasing temperature, confirming the typical ductile-to-brittle transition behavior of HSLA steels. Response surface methodology was applied to model the variation of absorbed energy as a function of the studied parameters. A first-order interaction model was developed to correlate the experimental parameters (T, Nd) with the fracture energy (U) and to predict its values within the investigated domain. The obtained results contribute to a better assessment of the structural integrity of pipelines under different operating conditions.

Key words: pipelines, temperature, notch depth, Charpy impact test, response surfaces

1. Introduction

The development of fracture mechanics in the 1960s made it possible to design structures in which the concept of a present defect was an integral part of the structural calculations. As a result, an intrinsic material parameter, toughness, was highlighted to characterize its resistance to fracture. Toughness is conventionally measured using standardized test specimens. Structural steels exhibit a ductile-brittle transition in both toughness and fracture resistance with increasing temperature. The brittle fracture toughness of these steels plays a vital role in certifying the safety of important industrial structures, such as oil power plants. These steels are characterized by a high elastic limit, excellent resilience at low temperatures, and good aptitude for weldability and forming [1, 2]. HSLA steels can be processed using all mechanical cutting processes, including laser and high-definition plasma cutting [3]. The AFNOR standards (NF-03508) set tolerances on the geometric elements of the machine; their variations must help better understand and control the dispersion observed during tests [4]. The test consists of imposing a shock directly above the notch, with the specimen being held by two supports on the opposite face to cause crack opening. A CHARPY pendulum hammer [5] is used for this. The Charpy V-notch test is intended to provide a simplistic measure of the material's ability to absorb energy when subjected to impact loading [6]. The transition from ductile fracture at high temperatures to brittle fracture at very low temperatures is a characteristic that must be carefully examined, as it is the cause of many accidents. Hence, understanding the evolution of resilience as a function of temperature is of significant importance [7]. Designs of experiments (DOE) provide many advantages for the design and analysis of experiments. First, they allow for the exploration of a large number of factors and levels within a limited number of trials, saving time, resources, and costs. DOE also makes it possible to determine the individual effects of each factor as well as the interactions between them,

*Corresponding author: e-mail addresses: s.achouri@crti.dz, souma_sihem@yahoo.fr

helping to identify the most influential variables on the responses studied [8]. Another advantage of DOE is the ability to use graphical representations to visualize relationships between input variables and responses. These visual tools, such as contour plots or three-dimensional plots, facilitate understanding of complex factor-response relationships [9]. Additionally, DOE allows the use of mathematical models to describe and predict these relationships, which can be leveraged to optimize input parameters and achieve specific goals. For example, optimization techniques can be applied to find experimental conditions that maximize yield or minimize cost [10]. Several experimental design methods are available, including full factorial design, fractional factorial design, central composite design, and Taguchi design, among others. The choice of the appropriate experimental design depends on the objectives of the experiment, the number of factors to be studied, and the experimental constraints [11]. The techniques for characterizing the impact resistance of materials remain debated and do not present clear objectivity. Initially, impact resistance was characterized by impact tests where the determined parameter was the energy lost by the hammer per unit area of the specimen [12, 13]. Current studies indicate that this energy does not always represent the critical fracture energy [14]. C. E. Turner and J. G. Williams [15, 16] proposed a method for interpreting impact tests based on fracture mechanics, known as the compliance method. Using this approach, a series of impact tests on notched specimens allows for the determination of the material's intrinsic fracture energy. The goal of this experimental and numerical study is to evaluate the Charpy impact test toughness of API 5L X70 steel, commonly used in pipeline construction. The objective of this work is therefore to experimentally and statistically investigate the combined influence of temperature and notch depth on the Charpy impact toughness of API 5L X70 steel. A factorial experimental design coupled with regression modeling is employed to establish predictive relationships between process parameters and absorbed fracture energy.

Fig. 1. Cut samples: (a) pipe cutting, (b) ferrule, and (c) specimen.

2. Material and method

2.1. Chemical composition

The material utilized for the purpose of conducting this experimental study is a carbon steel that is commonly employed in the transportation of hydrocarbons. This particular type of carbon steel is known as API 5L X70, which corresponds to its classifica-

Table 1. Chemical composition of API 5L X70 steel (wt.%)

C	Si	Mn	S	P	Cr	Nb	Ni	Ti	Fe
0.123	0.27	1.68	0.005	0.012	0.051	0.033	0.04	0.03	Ball.

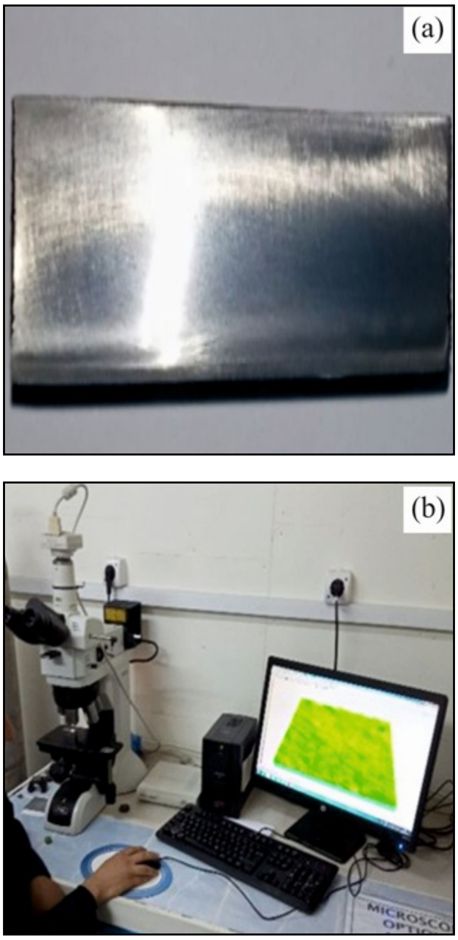

Fig. 2. NIKON Optical Microscope: (a) polished specimen and (b) microstructure observation.

tion according to the API5L standard. The chemical composition of this steel is provided in Table 1.

2.2. Sample preparation

A ferrule of 1.5 to 2 times the diameter of the tube is cut from the end of the tube; then a tongue in the longitudinal direction is sawn along the ferrule. The study was conducted on X70 steel specimens extracted from a tube. The cutting was carried out using a metallographic chainsaw (Fig. 1). The samples underwent mechanical polishing using a polisher under continuous lubrication (water jet) to avoid any local heating due to friction, using abrasive papers of different grain sizes.

2.3. Metallographic observations

The microstructural characterization was performed by optical microscopy using a NIKON microscope (Fig. 2).

A section in the plane perpendicular to the axis of the tube allowed us to observe the microstructure, which is essentially composed of grains of polygonal ferrite (white) and pearlite (dark), organized in bands. This type of microstructure is generated by the segregation of Mn and P elements during rolling; it is very common in X70 steels (Fig. 3).

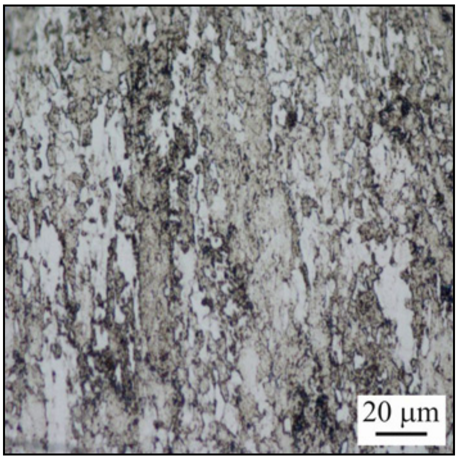

Fig. 3. Micrograph in cross section of pipe X70.

3. Experimental setup

3.1 Charpy shock machine

The impact tests were carried out using a FRANK 53580 pendulum hammer in accordance with the DIN 51222 standard. It is a question of determining the impact energy and impact resistance (resilience) of notched bars using the DIN standard, as illustrated in Fig. 4.

3.2. Climatic chamber

The climatic or thermal chamber located at URASM Annaba is depicted in the accompanying illustration. This specialized chamber allows temperature manipulation over a broad range, from a minimum of –10 to a maximum of 150 °C. The purpose of this chamber is to subject samples to varying temperatures and rates of heating or cooling, enabling precise control and experimentation with different materials (Fig. 5).

3.3. Standards used for the Charpy impact test

The specimens were precision-machined to comply with the geometric requirements specified in Figure 6 of ASTM E23 [17].

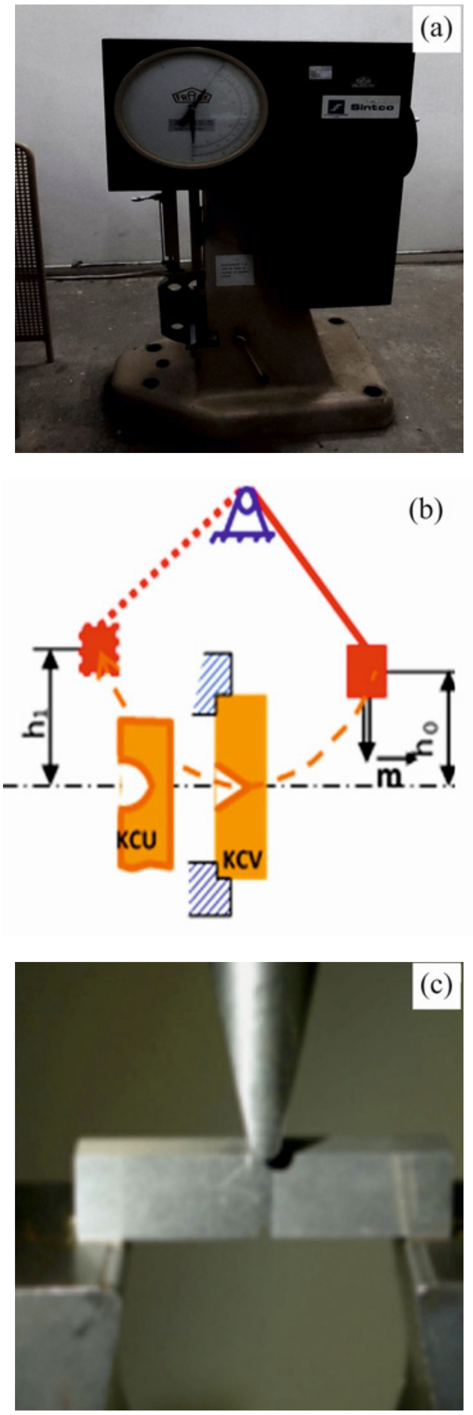

Fig. 4. KARLFRANK 300 Joule Pendulum Hammer (Type 53580) and (a) machine, and (b) schematic diagram, and (c) specimen supported on two anvils.

Fig. 5. Climatic chamber.

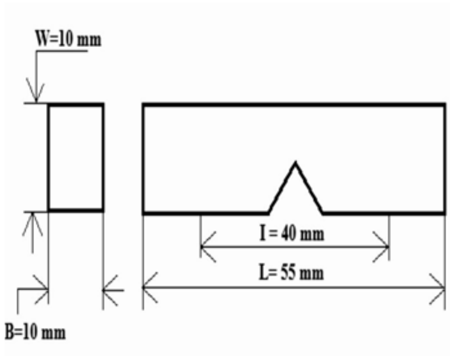

Fig. 6. Geometry and dimensions of the specimens.

4. Results

To evaluate the reliability and physical significance of the experimental results, a statistical analysis of the absorbed energy U was performed using the mean value (U_{moy}), standard deviation (e), and coefficient of variation (CV). These parameters allow quantification of both the central tendency and the dispersion of the experimental measurements at each testing temperature (Table 2):

$$U_{\text{moy}} = \sum U_i/n, \tag{1}$$

$$e = \sqrt{\left(\sum(U_i - U_{\text{moy}})/n\right)}, \tag{2}$$

$$CV = \frac{e}{U_{\text{moy}}} \times 100\%. \tag{3}$$

The average absorbed energy increases overall with increasing temperature, rising from 187 J at −10 ℃ to 230 J at 65 ℃. This trend indicates a progressive increase in material toughness with temperature.

The dispersion of results provides additional insight into the fracture mechanisms. At −10 ℃, the standard deviation is very low (± 3.33 J) with a coefficient of variation of only 1.78 %, demonstrating excellent repeatability and a stable fracture mode dominated by brittle behavior. In contrast, the highest

T a b l e 2. Measurement results

N	01	02	03	04	05	06	07	08	09	10	11	12
T (℃)	–10	–10	–10	0	0	0	25	25	25	65	65	65
η/Bb	0.16	0.18	0.17	0.14	0.12	0.11	0.13	0.15	0.16	0.13	0.10	0.12
U (J)	192	186	183	202	151	190	208	219	202	203	218	240
U_{moy} (J)		187			181			210			230	
Standard deviation, e		± 3.33			± 20			± 6.22			± 8	
Coefficient of variation, CV (%)		01.78			11.04			02.96			03.47	

dispersion occurs at 0 ℃, where the standard deviation reaches ± 20 J and the CV increase to 11.04 %. This significant variability confirms the presence of a transition regime in which fracture behavior becomes highly sensitive to microstructural heterogeneities and local stress conditions. Such variability is commonly associated with the coexistence of cleavage and ductile mechanisms.

At higher temperatures (25 and 65 ℃), the standard deviations decrease again (± 6.22 and ± 8 J, respectively), while the coefficients of variation remain low (2.96 and 3.47 %). These reduced dispersion levels indicate a more homogeneous deformation process and stable ductile fracture propagation. The simultaneous increase in absorbed energy and reduction in relative variability confirms improved energy dissipation capability and mechanical stability of the material.

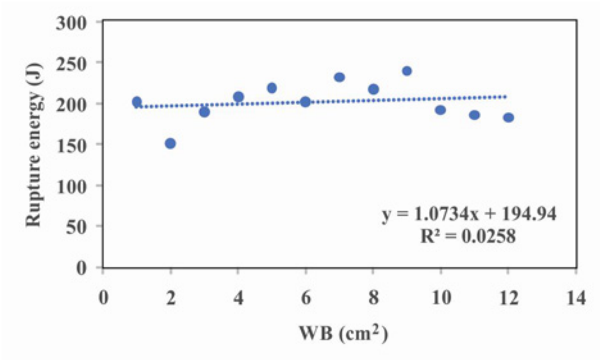

Fig. 7. Evolution of the rupture energy according to the parameters of the energy criterion.

The increase in the total energy of the rupture with the increase in the ruptured surfaces results in the fact that the rupture is an energy-consuming phenomenon. Therefore, the increase in broken surfaces requires more energy. The slope of the curve U (Bb) makes it possible to determine the critical energy of rupture or force of extension of the crack in mode I noted KCV.

This effect of distribution of the different stresses between the two stresses combined with a size effect are one of the consequences of the differences observed in the values of the mechanical characteristics.

In the tested samples, the fracture energy was observed to increase with rising temperature. Conversely, a slight decrease in absorbed energy was observed with decreasing temperature. A slight deviation was noted at 10 ℃; however, the overall trend clearly indicates an increase in fracture energy with rising temperature.

The purpose of the impact test, conducted according to ASTM E23, is to evaluate the material's resistance to dynamic fracture through the measurement of absorbed impact energy.

The purpose of the impact test is to determine the resistance of materials to rupture under the effect of an impact via the energy of rupture.

Structural defects act as stress concentrators, inducing a notch effect that locally modifies the stress field and increases stress triaxiality. Under such conditions, metals that are initially ductile may experience embrittlement, particularly after prolonged exposure to elevated temperatures, which promotes grain growth, grain-boundary precipitation, and the formation of brittle phases that reduce fracture resistance [18].

This variability in the mechanical response of materials is an experimental fact thatshould be taken into account in the calculations for the dimensioning of parts and structures made with these materials. [19, 20].

The fracture energy displayed a clear temperature dependence, particularly around the ductile-to-brittle transition temperature (Fig.7). As the temperature increased, the energy required for fracture also increased, consistent with findings from prior studies by Depraetere et al. and Mohammadi et al. [21, 22].

The results demonstrated that the notch depth (Nd) had a significant effect on fracture energy. At elevated temperatures, a smaller notch depth led to greater energy absorption, underscoring the critical influence of notch depth on fracture behavior. This observation aligns with recent work by Dehghanipoodeh et al. and other studies by Achouri [23, 24].

Fracture energy was found to correlate with the rupture surface area, which expanded with an increase in notch depth, requiring more energy for fracture. This behavior highlights the energy consumption dur-

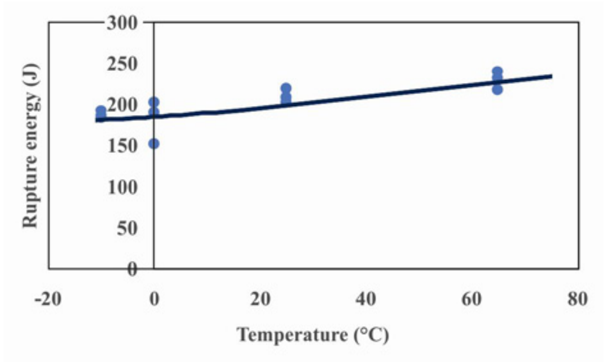

Fig. 8. Evolution of the rupture energy as a function of temperature.

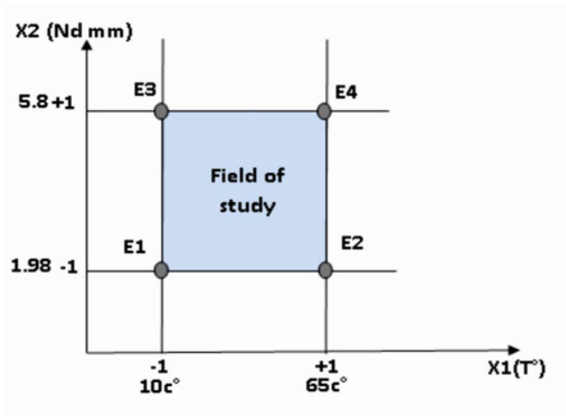

Fig. 9. Principle of the experiment.

ing fracture propagation and its connection to the stress distribution. and notch geometry, which has been extensively studied of Hosseinzadeh et al. and Soderholm [25, 26].

4.1. Modeling and statistical analysis

Factorial designs are a powerful tool for conducting experiments efficiently while obtaining maximum information. In this particular case, the use of a 2^2 factorial design allowed for the manipulation of two factors at two levels (–1, +1) in a total of four experimental conditions. The factorial design method is based on mathematical rules and allows for the systematic manipulation of multiple factors at different levels to determine their effects on a dependent variable. The use of two factors in this design allows for the identification of main effects, which are the effects of each factor on the dependent variable, as well as interaction effects, which are the combined effects of both factors on the dependent variable.

To make the conduct of the tests easier, the experimental design method was adopted, in this case the factorial designs. This technique makes it possible to minimize the number of experiments while having the maximum of information which helps to save time and to save the raw material. Designs of experiments are based on mathematical rules. The experimental tests were carried out according to the factorial plans 2^2 composed of two factors at two levels (–1, +1) (Fig. 9). The mathematical model postulated is a first-degree polynomial model with interactions presented in Eq. (4):

$$Y = a_0 + a_1X_1 + a_2X_2 + a_{12}X_1X_2, \quad (4)$$

where a_0 is a constant coefficient of the model, a_1 is a coefficient of factor 1, a_2 is a coefficient of factor 2, and a_{12} is a coefficient of factor X_1X_2.

In this experimental part, Charpy impact tests were carried out using notched specimens and were conducted in accordance with the following condition: $0.2 < a/w < 0.6$ [27]. Its tests were conducted at two temperatures (25 and 65 ℃). To study the toughness of X70 steel by varying the temperature and the notch depth (Nd).

Table 3. Experience matrix table

Test $N°$	Codes factor		Input parameters	
	X_1	X_2	T (℃)	Nd (mm)
E1	−1	−1	−10	1.98
E2	+1	−1	+65	1.98
E3	−1	+1	−10	5.8
E4	+1	+1	+65	5.8

Table 4. Matrix of experiment and results of energy U

Test $N°$	Input parameters		Output parameter
	T (℃)	Nd (mm)	U(J)
E1	–10	1.98	186
E2	65	1.98	240
E3	–10	5.8	101
E4	65	5.8	134

4.2. Mathematical models statistical analysis

The postulated model of the complete factorial plans 2^2 is of the following form (Eq 5):

$$U = a_0 + a_1X_1 + a_2X_2 + a_{12}X_1X_2, \quad (5)$$

where X_1 represents the level of the factor 1, X_2 rep-

Table 5. Polynomial coefficient values for U

Polynomial coefficient	U (J)
a_0	165.25
a_1	21.75
a_2	–47.75
a_{12}	–5.25

resents the level of the factor 2, X_1X_2 is the product of the factor levels 1 et 2, a_0 is the constant coefficient of the model, a_1 is the coefficient of the factor X_1, a_2 is the coefficient of the factor X_2, and a_{12} is the coefficient of the term X_1X_2 (see Eqs. (6)–(9)):

$$a_0 = 1/4[y_1 + y_2 + y_3 + y_4], \quad (6)$$

$$a_1 = 1/4[-y_1 + y_2 - y_3 + y_4], \quad (7)$$

$$a_2 = 1/4[-y_1 + y_2 + y_3 + y_4], \quad (8)$$

$$a_{12} = 1/4[y_1 - y_2 - y_3 + y_4]. \quad (9)$$

After calculating the polynomial coefficients for each answer, the values are recorded in Table 5.

4.3. Output response modeling

The correlation between the input parameters (temperature T and the notch depth Nd) and the output response in this case the energy was obtained by linear regression which is illustrated by the Eq. (7). Furthermore, it makes it possible to predict the output responses (U) at any point in the study domain covered by the factors X_1 (for T) and X_2 (for Nd):

$$U = 165.25 + 21.75X_1 - 47.75X_2 - 5.25X_1X_2, \quad (10)$$

$$U(J) = 238.7 + 0.8651T - 22.89Nd - 0.07330T \times Nd. \quad (11)$$

Statistical analysis shows that the residual energy U follows a straight line (Fig. 10) showing no asymmetry. The distribution curve of the residuals indicates that their distribution is random with respect to zero and without singular predisposition hence the established model explains the experimental results well.

4.4. Effect of interactions on responses (3D plots and contours)

The response surfaces (Fig. 11). Illustrate the variation of the response studied in this case, the absorbed energy (U) as a function of the temperature (T) and the notch depth (Nd). The graph shows that the effect of the depth of the notch depth (Nd) on the variation of the energy U is more significant than the effect of the temperature, where it clearly appears that the energy reaches its maximum ($U = 250$ J) for a minimum

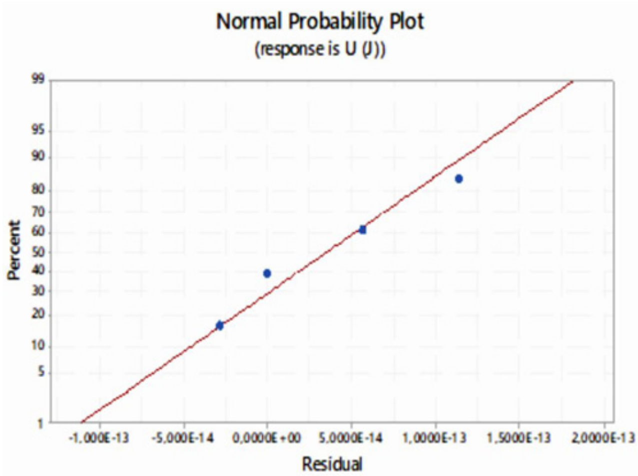

Fig. 10. Curve of the residuals.

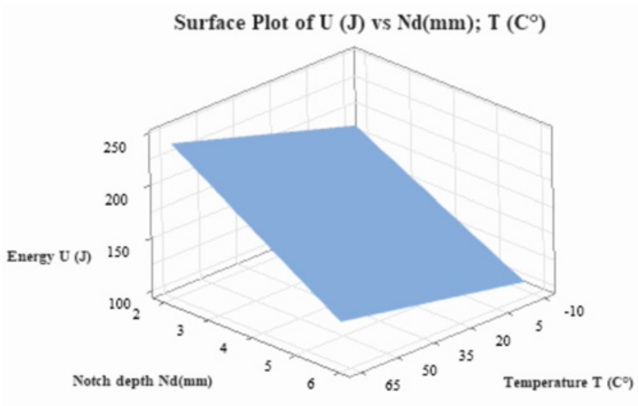

Fig. 11. Variation of the response studied the absorbed energy (U) as a function of the temperature (T) and the notch depth (Nd)

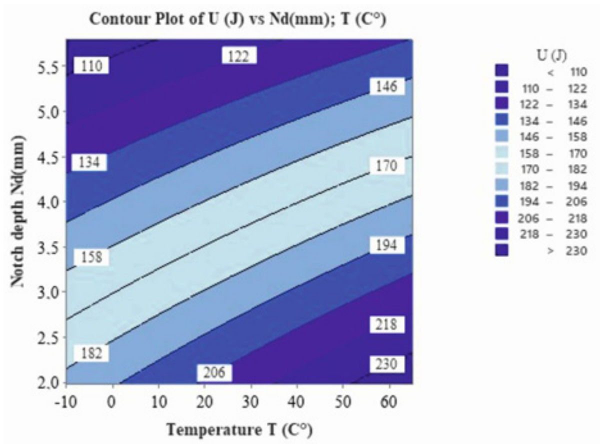

Fig. 12. Graphic contours of the response surface.

notch depth ($Nd = 1.98$ mm) associated with a maximum temperature ($T = 65$ ℃). Whereas, for a notch

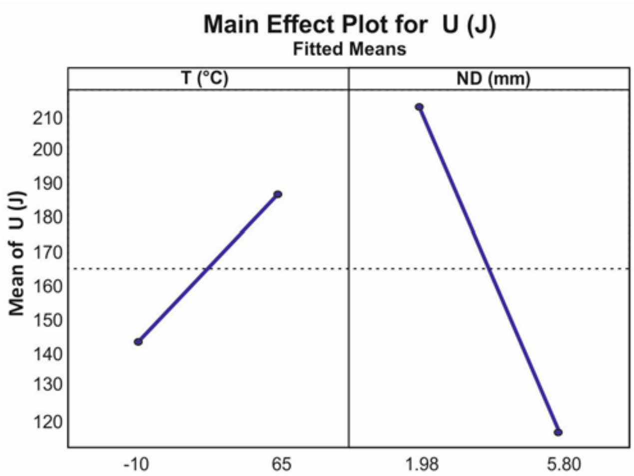

Fig. 13. Effect of the two input parameters.

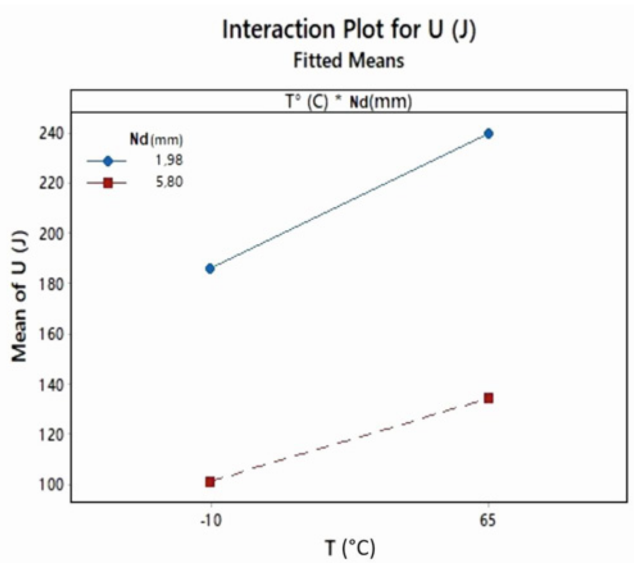

Fig. 14. Interaction curve.

depth at its maximum level, the energy is practically constant and varies between 101 and 134 J, regardless of temperature.

Furthermore, Fig. 12 shows the graphic contours of the response surface, which also make it possible to deduce the values of the response U. These contours show the relationship between a response value U and two input factors (Nd, T). Points with the same answer are joined to generate contour lines consistent with the answers.

Figure 13 indicates the effect of the two input parameters (Nd, T) on the energy U, where the curve shows a higher slope, indicating that the factor Nd has a greater influence on the response with respect to temperature T, from which we can deduce that the cut face greatly affects the absorbed energy U. Moreover, the interaction curve (Fig. 14) clearly reveals there is no visible interaction between the two input parameters (Nd, T).

5. Conclusion

This work analyzed the combined effects of temperature and notch depth on the Charpy impact toughness of API 5L X70 pipeline steel by combining an experimental approach with statistical modeling based on design of experiments (DOE). The main findings can be summarized as follows:

– The absorbed fracture energy increases with temperature, confirming the ductile-brittle transition behavior characteristic of high-strength low-alloy (HSLA) steels.

– The notch depth has a more pronounced influence on the absorbed energy than temperature within the studied range. In particular, increasing the notch depth leads to a decrease in fracture energy, indicating a higher sensitivity to crack initiation and propagation.

– The developed model established a quantitative relationship between the studied parameters (T, Nd) and the fracture energy (U), making it possible to predict the response within the investigated experimental domain.

– The statistical analysis confirms the reliability of the experimental results, particularly through the low values of the coefficient of variation observed outside the ductile-brittle transition region.

– The effect and interaction curves highlight the significant influence of the parameters (T, Nd) on the studied response (U).

– According to the iso-response and contour plots, the maximum energy ($U = 250$ J) is obtained for the minimum notch depth ($Nd = 1.98$ mm) combined with the highest temperature ($T = 65$ °C).

Overall, the approach combining design of experiments and response surface methodology proves to be an effective tool for analyzing and predicting fracture behavior and for assessing the structural integrity of pipeline steels.

Future work should extend the analysis to nonlinear modeling and broader temperature ranges in order to further improve the predictive capability of the developed model.

References

[1] R. W. Fonda, G. Spanos, Microstructural evolution in ultra-low-carbon steel weldments – Part I: Controlled thermal cycling and continuous cooling transformation diagram of the weld metal, Metall. Mater. Trans. A 31 (2000) 2145–2153. https://doi.org/10.1007/s11661-000-0132-0

[2] W. Chen, L. Liang, B. Zhou, J. Ye, X. Sun, J. Ma, J. Yu, K. Yu, A fracture mechanics model for predicting tensile strength and fracture toughness of 3D printed engineered cementitious composites (3DP-ECC), Eng. Fract. Mech. 316 (2025) 110894. https://doi.org/10.1016/j.engfracmech.2025.110894

[3] T. Bakke, J. Klungsøyr, S. Sanni, Environmental impacts of produced water and drilling waste discharges from the Norwegian offshore petroleum industry, Mar. Environ. Res. 92 (2013) 154–169. https://doi.org/10.1016/j.marenvres.2013.09.012

[4] M. Reytier, S. Chapuliot, S. Marie, L. Ferry, M. Nedelec, Study of cleavage initiation under thermal shock by tests on cracked rings and thermomechanical calculations, Nucl. Eng. Des. 236 (2006) 1039–1050. https://doi.org/10.1016/j.nucengdes.2005.10.007

[5] B. Jacquot, Mechanical properties of biomaterials used in dentistry, French-Speaking Society of Dental Biomaterials (SFBD), French-Speaking Virtual Medical University 2010. (in French)

[6] F. Di Gioacchino, E. Lucon, E. B. Mitchell, K. D. Clarke, D. K. Matlock, Side-grooved Charpy impact testing: Assessment of splitting and fracture properties of high-toughness plate steels, Eng. Fract. Mech. 252 (2021) 107842. https://doi.org/10.1016/j.engfracmech.2021.107842

[7] M. Fang, K. Wang, H. Lu, Y. Yang, S. Nutt, Covalent polymer functionalization of graphene nanosheets and mechanical properties of composites, J. Mater. Chem. 19 (2009) 7098–7105. https://doi.org/10.1039/B908220D

[8] D. C. Montgomery, Design and Analysis of Experiments, John Wiley & Sons, 2017. ISBN: 9781119113478(PBK), ISBN:9781119299455(EVALC)

[9] R. H. Myers, D. C. Montgomery, C. M. Anderson-Cook, Response Surface Methodology: Process and Product Optimization Using Designed Experiments, John Wiley & Sons, 2016. https://doi.org/10.1080/15458830.1996.11770760

[10] B. C. Y. Lee, M. S. Mahtab, T. H. Neo, I. H. Farooqi, A. Khursheed, A comprehensive review of design of experiment (DOE) for water and wastewater treatment application, J. Water Process Eng. 47 (2022) 102673. https://doi.org/10.1016/j.jwpe.2022.102673

[11] A. I. Khuri, J. A. Cornell, Response Surfaces: Designs and Analyses, CRC Press, 2018. https://doi.org/10.1201/9780203740774

[12] W. Xu, S. I. Thorsson, A. M. Waas, Experimental and numerical study on cross-ply woven textile composite with notches and cracks, Compos. Struct. 132 (2015) 816–824. https://doi.org/10.1016/j.compstruct.2015.06.067

[13] M. Dutkiewicz, O. Hembara, O. Chepil, M. Hrynenko, T. Hembara, A new energy approach to predicting fracture resistance in metals, Materials 16 (2023) 1566. https://doi.org/10.3390/ma16041566

[14] F. Berto, Fatigue and fracture assessment of notched components by means of the strain energy density, Eng. Fract. Mech. 167 (2016) 176–187. https://doi.org/10.1016/j.engfracmech.2016.04.021

[15] C. E. Turner, Comparison of dynamic test proposals: Some UK experience on testing at intermediate rates, Remarks on the interpretation of instrumented Charpy-type impact tests, 1981.

[16] J. G. Williams, Fracture mechanics of polymers, Polym. Eng. Sci. 17 (1977) 144–149. https://doi.org/10.1002/pen.760170303

[17] R. Chaouadi, R. Gerard, Development of a method for extracting fracture toughness from instrumented Charpy impact tests in the ductile and transition regimes, Theor. Appl. Fract. Mech. 115 (2021) 103080. https://doi.org/10.1016/j.tafmec.2021.103080

[18] J. Peng, Y. Wang, Q. Dai, X. Liu, L. Liu, Z. Zhang, Effect of stress triaxiality on plastic damage evolution and failure mode for 316L notched specimen, Metals 9 (2019) 1067. https://doi.org/10.3390/met9101067

[19] E. N. Shaqour, The impact of adopting lean construction in Egypt: Level of knowledge, application, and benefits, Ain Shams Eng. J. 13 (2022) 101551. https://doi.org/10.1016/j.asej.2021.07.005

[20] Y. Bao, Dependence of ductile crack formation in tensile tests on stress triaxiality, stress and strain ratios, Eng. Fract. Mech. 72 (2005) 505–522. https://doi.org/10.1016/j.engfracmech.2004.04.012

[21] R. Depraetere, W. De Waele, M. Cauwels, T. Depover, K. Verbeken, M. Boone, S. Hertelé, Influence of stress triaxiality on hydrogen assisted ductile damage in an X70 pipeline steel, Mater. Sci. Eng. A 864 (2023) 144549. https://doi.org/10.1016/j.msea.2022.144549

[22] A. H. Mohammadi, M. Naderi, M. Iranmanesh, Fracture toughness evaluation of 3Cr-1Mo steel from Vickers indentation and tensile test data, Procedia Eng. 10 (2011) 228–235. https://doi.org/10.1016/j.proeng.2011.04.041

[23] M. Dehghanipoodeh, J. Hashemi, H. Valipour, H. Masoumi, Effect of notch corner shapes on mechanical behaviour and failure mechanism of notched timber beams, Constr. Build. Mater. 447 (2024) 138085. https://doi.org/10.1016/j.conbuildmat.2024.138085

[24] S. Achouri, M. Bourebia, S. Meddah, A. Oulabbas, B. Redjel, Study of the toughness of a composite material as a function of variation in notch geometry, architecture, and molding flow, Mech. Compos. Mater. (2025) 1–12. https://doi.org/10.1007/s11029-025-10252-3

[25] A. Hosseinzadeh, S. H. Hashemi, H. Rastegari, M. R. Maraki, Investigation of the notch depth effect on Charpy fracture energy and fracture surface features of API X65 steel, Can. Metall. Q. 62 (2023) 36–48. https://doi.org/10.1080/00084433.2022.2066241

[26] K. J. Soderholm, Review of the fracture toughness approach, Dent. Mater. 26 (2010) e63–e77. https://doi.org/10.1016/j.dental.2009.11.151

[27] R. Smith, A Mechanistic Modelling Approach To Derive Fracture Toughness Properties From Charpy Impact Energy In The Lower Transition Region. (EngD Thesis), The University of Manchester, United Kingdom, 2015.